

Study of the GaAs surface oxide desorption process by annealing in ultra high vacuum conditions

M. López-López, A. Guillén-Cervantes, Z. Rivera-Alvarez, E. López-Luna, and I. Hernández-Calderón
*Physics Department, Centro de Investigación y Estudios Avanzados del Instituto Politécnico Nacional
Apartado postal 14-740, 07000 México, D.F., Mexico*

Recibido el 15 de abril de 1999; aceptado el 3 de diciembre de 1999

We have studied the desorption mechanism of Ga- and As-oxides on GaAs (100) by subjecting the substrates to two thermal processes in ultra high vacuum (UHV) conditions. The first process was an outgassing at 350°C, and the second process consisted of an annealing at 530°C. The pressure variations in the UHV chambers recorded during both thermal treatments showed a behavior related to the removal of As- and Ga-oxides from the substrate surface. The thermally treated GaAs (100) substrates were analyzed by *in-situ* reflection high-energy electron diffraction (RHEED), Auger electron spectroscopy, and *ex-situ* atomic force microscopy (AFM). The samples before the oxide removal showed a diffuse RHEED image with intense background, characteristic of an amorphous material. In contrast the RHEED patterns of substrates after the oxide desorption process were streaky and well defined indicating a high quality surface. AFM images clearly showed the presence of surface pits on the GaAs(100) samples exposed to the high temperature oxide desorption process. The pits have a density in the order of $10^9/\text{cm}^2$, and some are as deep as 120 Å. We explain the pits formation mechanism in terms of chemical reactions of the surface oxides with the elements of the substrate. We found that pits are generated at temperatures as low as 350°C, which coincides with the desorption of the most unstable oxides, presumably As-oxides.

Keywords: GaAs; surface oxides; molecular beam epitaxy

En este trabajo se estudia el mecanismo de evaporación de los óxidos de Ga y As en sustratos de GaAs(100). Los sustratos se sometieron a dos procesos térmicos en condiciones de ultra alto vacío (UAV). El primer proceso fue un degasado a 350°C, mientras que el segundo proceso consistió en un recocido a 530°C. Las variaciones en las presiones de las cámaras de UAV se grabaron durante los dos tratamientos térmicos, estas variaciones mostraron un comportamiento correlacionado con la remoción de óxidos de Ga y As de la superficie del sustrato. Los sustratos de GaAs tratados térmicamente se analizaron *in-situ* por medio de difracción de electrones de alta energía y espectroscopía electrónica Auger. Además se realizó un estudio *ex-situ* por medio de microscopía de fuerza atómica (MFA). Las muestras antes de la evaporación de los óxidos mostraron una imagen de difracción de electrones difusa, característica de un material amorfo. En contraste, los patrones de difracción de electrones de los sustratos después de la evaporación de los óxidos mostraron líneas bien definidas indicando una superficie de buena calidad cristalina. Las imágenes de MFA mostraron claramente la presencia de huecos en la superficie de los sustratos de GaAs(100) sujetos al proceso de evaporación de los óxidos a alta temperatura. Estos huecos se presentan con una densidad del orden de $10^9/\text{cm}^2$, y con una profundidad de 120 Å. Explicamos el mecanismo de formación de estos huecos en términos de reacciones químicas de los óxidos con el sustrato de GaAs. Se encontró que estos huecos se comienzan a generar a temperaturas bajas ($\sim 350^\circ\text{C}$), que coinciden con las temperaturas a las cuales se evaporan los óxidos de arsénico más inestables.

Descriptores: GaAs; óxidos de Ga y As; epitaxia por haces moleculares

PACS: 81.05.Ea; 81.15.Hi; 61.14.Hg

1. Introduction

Obtaining high quality GaAs surfaces with good structural properties is a key issue in the development of high speed and optoelectronics device technology, in which GaAs wafers are commonly used as substrates. In the last decade GaAs has been also considered a prominent substrate for engineering optical devices such as II-VI blue-green lasers by molecular beam epitaxy (MBE) growth techniques [1].

It has been reported that the initial GaAs surface condition directly affects the II-VI epitaxy [2]. Thus, in order to succeed in developing the above mentioned devices, a starting high quality GaAs surface prior to the growth must be assured [3]. With this purpose, GaAs substrates are treated under different cleaning processes trying to obtain a substrate surface as defect- and contaminant-free as possible.

Typically, the substrate preparation method before the MBE growth consists of an *ex-situ* chemical etching of the GaAs surface to produce fresh oxides, then an outgassing process and, as a final stage a thermal treatment under ultra high vacuum (UHV) conditions in order to remove the surface oxides. The understanding of the physical and chemical phenomena occurring during the oxides desorption is necessary to develop surface treatments for the complete removal of these oxides and other contaminants, which is extremely important to obtain a high quality epitaxial layer.

In this work, the oxides desorption mechanism on GaAs(100) surfaces was studied by *in-situ* reflection high-energy electron diffraction (RHEED), Auger electron spectroscopy (AES), and *ex-situ* atomic force microscopy (AFM). Two important changes on the GaAs surface were observed: an increase in roughening after the thermal cleaning process,

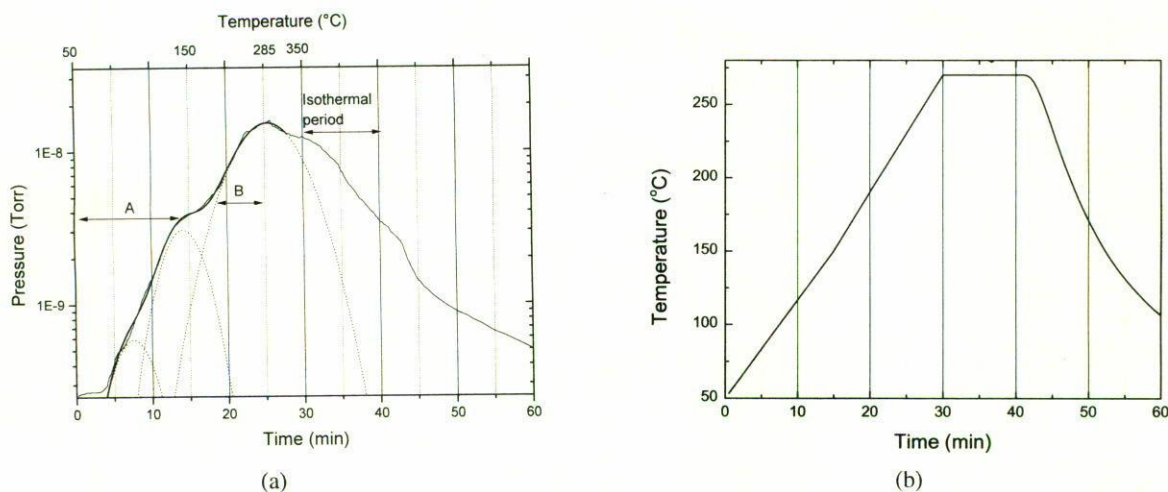


FIGURE 1. (a) Pressure curve obtained during the outgassing process of a GaAs (100) substrate using the temperature profile shown in (b).

and the generation of pits on the surface of the GaAs samples. These morphological changes are due to a stoichiometric degradation of the GaAs surface induced by the oxide desorption process. Surface oxides during the thermal treatment react with the underlying Ga and As atoms leading to surface erosion. As a result pits are generated in a density of $10^9/\text{cm}^2$. AFM measurements showed that pits can be as deep as 120 Å. For the first time we present evidence that shows that the surface pits are closely related to the sublimation of the most unstable oxides at temperatures as low as $\sim 350^\circ\text{C}$. The pressure variations registered during the outgassing process support these results.

2. Experimental procedures

Semi-insulating GaAs (100) undoped wafers were used in the experiments. The GaAs substrates were chemically etched in an $\text{H}_2\text{SO}_4 : \text{H}_2\text{O}_2 : \text{H}_2\text{O}$ (3:1:1) solution @ 60°C for 90 sec. After the etching, the substrates were rinsed in flowing deionized water ($10^{18} \text{ M}\Omega$) for 15 min and blown dry with N_2 under clean-room conditions. Finally, GaAs substrates were soldered with In to molybdenum blocks and loaded in a Riber 32P MBE system. This system comprises four UHV chambers: sample loading, sample preparation, MBE growth, and analysis. The substrates were first subjected to a thermal outgassing and then to an oxide removal process.

The outgassing process was carried out in the preparation chamber, substrates were heated up to $\sim 350^\circ\text{C}$ in UHV ($\sim 10^{-11}$ Torr) following a computer program. This program includes two temperature ramps. The first one increases the substrate temperature at a rate of $0.11^\circ\text{C}/\text{sec}$, in the range between 50 and 150°C . For the second ramp, the rate is $0.22^\circ\text{C}/\text{sec}$ going from 150 to 350°C . At the end of these ramps the substrate temperature is kept at $\sim 350^\circ\text{C}$ for 10 min. During this process the pressure variation in the chamber are monitored by an ion gauge and an analog recorder.

After this initial treatment, the samples are transferred into the growth chamber, with a base pressure of 10^{-11} Torr. The GaAs samples are heated, via a computer program, up to $\sim 530^\circ\text{C}$. Starting at 200°C , the temperature is increased at a rate of $0.32^\circ\text{C}/\text{sec}$ up to 350°C , and then at a $0.2^\circ\text{C}/\text{sec}$ until reaching 530°C . At this temperature an isothermal period completes the oxide desorption process. Throughout the whole oxide desorption the pressure variations in the chamber are registered as explained before.

Auger spectra were taken in the analysis chamber on the as-loaded samples, then after the outgassing, and finally after the oxide desorption process. The oxide desorption process was carefully monitored by *in-situ* RHEED. The diffraction patterns were recorded and analyzed by an image processor software. The substrate surface was studied at different stages of the oxide desorption by AFM *in-air*.

3. Results

Figure 1a shows the pressure variations (thin-solid line) in the preparation chamber recorded during the outgassing process, while Fig. 1b is the temperature profile applied to the GaAs samples in this process. It is important to mention the reproducibility of the pressure curve presented in the Fig. 1a, it is practically the same for every GaAs sample we have studied.

From Fig. 1a, a significant increase in the pressure can be observed for the first 15 min of the treatment, when the substrate temperature goes from 50 to $\sim 136^\circ\text{C}$ (the part in the curve identified with A). After this, the slope of the pressure curve decreases, indicated by the knee in the curve at the end of the region A. However, when the substrate temperature approaches to 190°C (18 min) the slope of the pressure increases and the pressure raises again (region B in the Fig. 1a). The experimental data of Fig. 1a in the ranges A and B were fitted to three gaussians. The sum of these gaussians reproduced very well the pressure behavior in the ranges A and B, as shown by the thick-solid line in Fig. 1a. The first

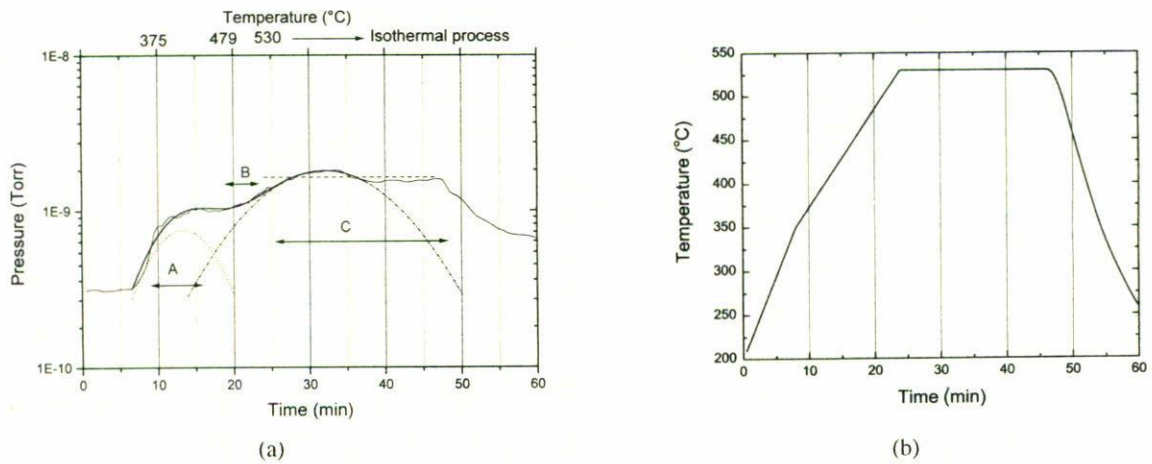


FIGURE 2. (a) Pressure behavior observed during the oxide desorption process of a GaAs (100) substrate. The temperature curve used in this process is shown in (b).

gaussian centered at about 100°C, is associated to evaporation of water molecules from the GaAs surface. The second and third peaks are centered at about 143 and 290°C, respectively. We will discuss in the next section the origin of these peaks. Note that from the pressure graph of the Fig. 1a, it is evident that the pressure is recovering during the isothermal period, this is an indication that no more volatile species are present on the GaAs surface at this temperature range.

The Fig. 2a shows the pressure curve (thin-solid line) recorded during the oxide desorption of the GaAs samples inside the MBE reactor. They were heated using the temperature profile of Fig. 2b. From Fig. 2a, we can observe important variations in the pressure curve for specific temperature ranges. In the temperature range from 355°C to 390°C (8 min to 11 min), the pressure increases rapidly and exhibits a peak in the region A shown in the Fig. 2a. The slope increases again after 20 min, as indicated in the region marked B in the graph. After this, the substrate enters into the isothermal period at a temperature of 530°C. It is interesting to note that despite that the temperature remains constant in this period, the pressure continues increasing and has a maximum in the region C. Then, from about 36 min to the end of the isothermal period the pressure remains almost constant. Finally, at the end of this period the pressure falls with the temperature. The maxima in the pressure curve were determined by fitting the data to two gaussians, as shown by the dotted lines in Fig. 2a. From the fitting, the first maximum occurs at 410°C, and the second at 33 min in the isothermal period (530°C). As we will explain in the next section, these peaks correspond to the evaporation of specific species from the substrate.

The desorption of oxides from the GaAs substrate ended when the pressure started to recover after the second peak (~35 min), as was confirmed by RHEED observations explained below. On the other hand, the horizontal dashed line in Fig. 2a shows the expected pressure due to Ga and As molecules evaporating from the GaAs surface at the temperature of 530°C, as obtained from reference [4]. This pressure is very close to that we observed ($\sim 1.5 \times 10^{-9}$ Torr) after

the last peak, therefore we think that during the rest of the isothermal period the constant pressure value is caused by the evaporation of Ga atoms and As molecules from the bare GaAs substrate.

Three-dimensional (3-D) AFM images of the GaAs surface at different stages of the thermal process are shown in the Fig. 3. The initial as-loaded GaAs surface is presented in the Fig. 3a, and Fig. 3b shows the GaAs substrate surface after the outgassing process at 350°C. The GaAs surface after the oxide desorption at 530°C is shown in the Fig. 3c. From these images it is important to note the GaAs surface has significantly changed after heating the samples. The most notorious change is the appearance of surface pits on the sample heated at 530°C. AFM line profiles were taken along the surface in order to quantitatively evaluate the morphological changes observed on the GaAs substrate. Typical profiles for the as-loaded, after outgassing, and after oxide desorption surfaces are shown in Figs. 4a, 4b, and 4c, respectively. The rms roughness value for the as-loaded surface is 1.3 Å, it increases to 3.6 Å after the outgassing, and the final value after the oxide desorption is 39 Å. The difference between the first two surfaces and the third is about one order of magnitude and is due to the contributions of the pits to the roughness statistics. One important point is that these pits have an elliptical shape, as observed in the AFM image of Fig. 5. Another interesting characteristic of these voids is their orientation. It was found that the main axis of the voids is along the $[0\bar{1}1]$ direction, while the minor axis lies on the $[011]$ direction. The voids can be as deep as 120 Å, with a density in the order of $10^9/\text{cm}^2$.

The RHEED patterns corresponding to the GaAs surfaces in the Figs. 3a, 3b, and 3c are shown in the Figs. 6a, 6b, and 6c, respectively. In Figs. 7a, 7b, and 7c we present intensity profiles of the RHEED patterns in Figs. 6a, 6b, and 6c, respectively. The halo RHEED image of the as-loaded surface showed in the Fig. 6a indicates that the oxide covers the substrate. Diffraction spots can not be observed from this surface (Fig. 7a), indicating that the oxide layer is amorphous. For the

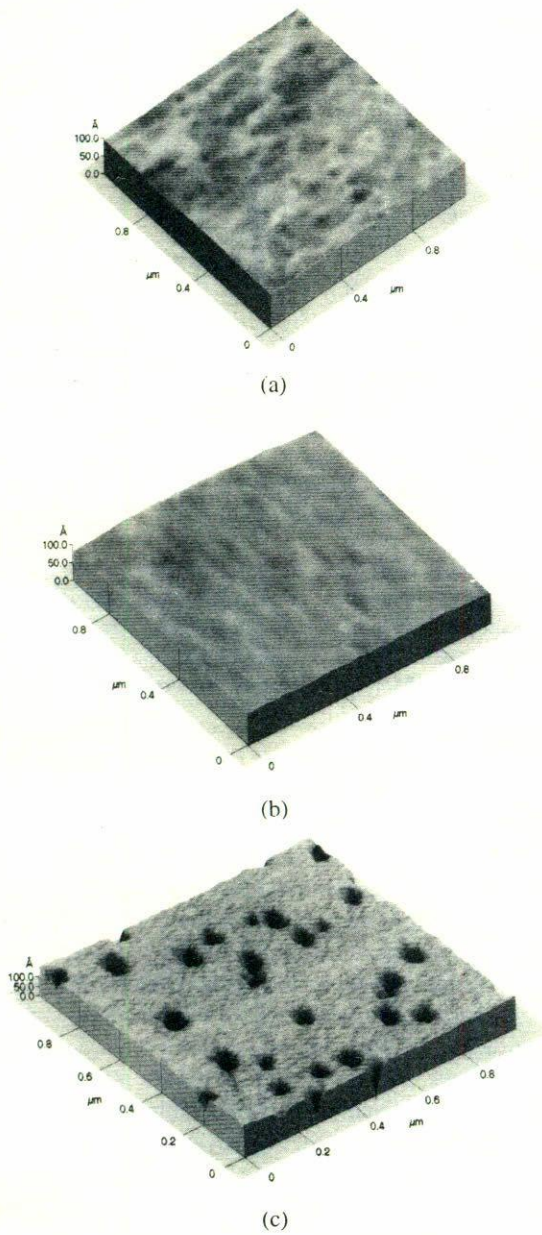


FIGURE 3. AFM images of: a) the initial as-loaded GaAs(100) surface, b) the GaAs surface after the outgassing process at 350°C, and c) the GaAs surface after the removal of the oxides at a temperature of 530°C.

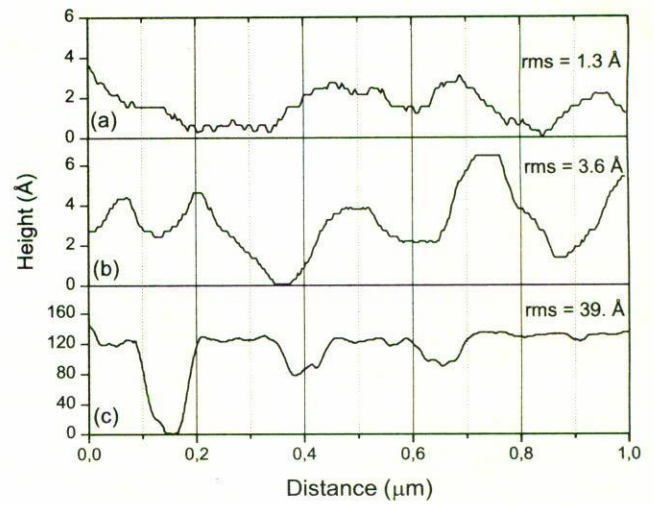


FIGURE 4. AFM line analysis of the same samples as in Fig. 3. The rms roughness values are: (a) 1.3 Å for the initial as-loaded surface, (b) 3.6 Å for the outgassed sample at 350°C, and (c) 39 Å for the GaAs surface after the removal of the oxides at a temperature of 530°C.

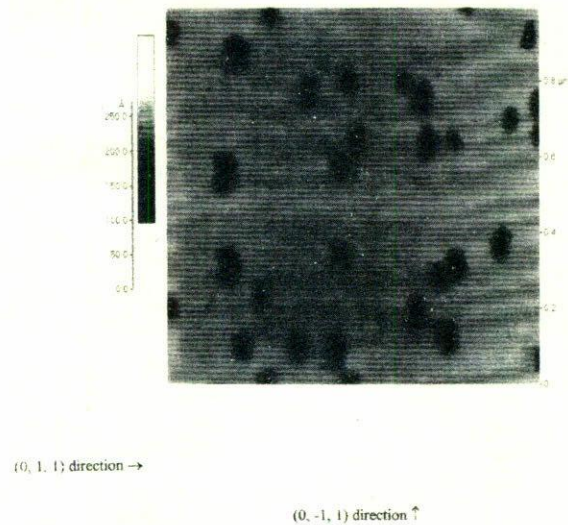


FIGURE 5. AFM plan view of the GaAs surface after the removal of the oxides. The elliptical shape of the pits formed is clearly observed.



FIGURE 6. RHEED patterns of: (a) the initial as-loaded GaAs(100) surface, (b) the GaAs surface after the outgassing process at 350°C, (c) the GaAs surface after the removal of the oxides at a temperature of 530°C.

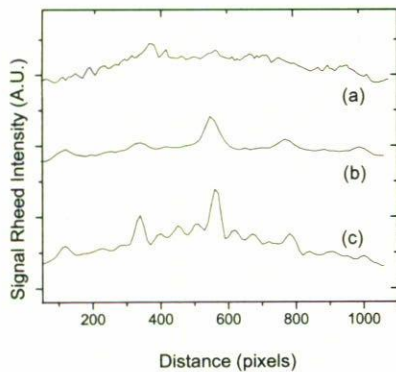


FIGURE 7. (a), (b), and (c) show intensity profiles of the corresponding RHEED patterns in Fig. 6.

sample outgassed at 350°C (Fig. 6b), we notice the appearance of GaAs bulk spots with a diffuse background, which indicates that a change in the sample surface has occurred. In the line analysis of Fig. 7b, the bulk streaks are cleared observed as broad peaks, however no reconstruction is present. In contrast, Fig. 6c shows a bright and well defined RHEED pattern of the GaAs surface after the oxide desorption at 530°C. This pattern exhibits a clear 4-fold reconstruction along the [011] direction, an indication of a Ga-rich GaAs surface [5]. The intensity profile in Fig. 7c clearly shows three intense peaks corresponding to the bulk streaks, and in between them we observe three smaller peaks, which correspond to the 4-fold reconstruction. With the help of Figs. 6 and 7 we can observe the transition from a GaAs surface initially covered with an amorphous layer of oxides to the final free-oxide single crystalline GaAs surface.

Figure 8a shows the AES peak ratios of O/As and O/Ga measured on the as-loaded sample, and at the end of each of the two thermal processes. Figure 8b shows the behavior of the Ga/As, Ga/(Ga+As), and As/(Ga+As) AES peaks ratios at different stages of the treatments. The AES results suggest that the structural and morphological changes observed by AFM and RHEED are closely related to changes in the chemical composition of the GaAs oxides, as will be discussed below.

4. Discussion

We will show that the initial composition of the GaAs oxides and the chemical reactions promoted by the thermal processes are responsible for the formation of surface pits shown in the Fig. 3c. Note that in spite of the small rms roughness value (3.6 Å) of the substrate outgassed at 350°C, it is evident that characteristic features have appeared on the surface, as compared to the initial as-loaded sample (Figs. 3b and 3a, respectively). Features similar to those final pits (Fig. 3c) are clearly observed in Fig. 3b, therefore we think that this AFM image shows the early stages of the pits formation. Apparently there are specific areas (precursors) on the outgassed GaAs substrate from which voids are finally outlined, we be-

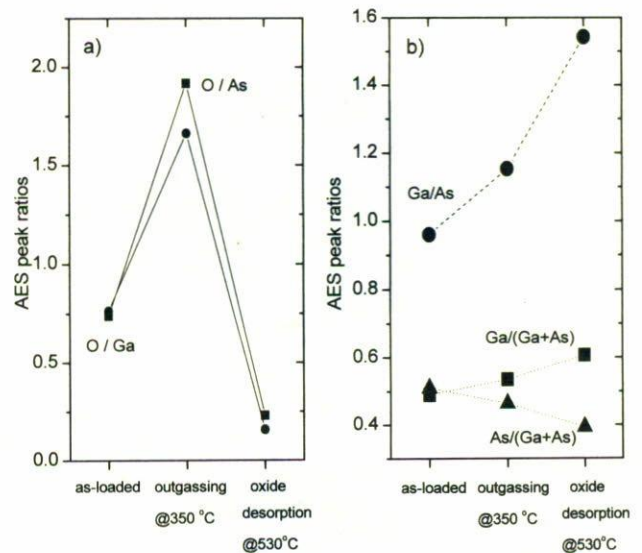


FIGURE 8. Auger peak intensity ratios measured at the end of the different thermal treatments. In (a) solid circles (●) and squares (■) indicate the O/Ga and O/As ratios, respectively. In (b) solid circles (●), squares (■) and triangles (▲) indicate the Ga/As, Ga/(Ga+As) and As/(Ga+As) ratios, respectively.

lieve that the chemical nature of these areas is related to the distribution of the most unstable oxides grown on the GaAs samples.

It has been reported that the initial oxidation on A^{III}-B^V materials involves formation of A-oxides as well as B-oxides islands growing at different rates [6, 7]. The general trend is that they grow locally and independently until they cover the whole surface of the semiconductor [6, 7]. Based on this growth model, oxides with different composition, and therefore with different sublimation temperatures coexist on the GaAs. Thus, highly volatile As-oxides may grow in the vicinity of thermodynamically more stable Ga-oxides, on the plane of the GaAs substrate. Moreover, the particular *ex-situ* treatments performed on our GaAs substrates result in the formation of a very thin (~ 10 Å) top most surface layer composed of very volatile As-oxides [8], and the accumulation of the most stable Ga-oxides (Ga₂O₃) near the GaAs surface [9, 10]. The total thickness of the GaAs oxides is about 40 Å [11]. This layer is thicker than the penetration depth of the electrons used in RHEED, and therefore diffraction spots from the GaAs crystal can not be observed in the as-loaded sample (Fig. 6a). As we will see the AES results will also reflect the effects of the GaAs oxide thickness.

First, we expect during the outgassing process the desorption of principally two different species from the substrate, which would lead to the second and third peaks in the pressure curve of Fig. 1a, respectively. First, the desorption of the top most surface layer of very volatile As-oxides, as well as other deeper volatile As-oxides like AsO, which has been detected at ~ 150 °C [8]. Therefore, we associate the second peak at 143°C observed in the pressure curve of Fig. 1a to the desorption of these volatile As-oxides. Then, when the tem-

perature further increases, chemical reactions between oxides and the GaAs surface are favored. For temperatures in the order of $\sim 300^\circ\text{C}$ the following reaction can be established [12–14]:



From this equation we note that the stable As-oxide As_2O_3 , reacts with the elements of the GaAs producing Ga_2O_3 , which is the most stable Ga-oxide. Also, as a result of this reaction arsenic molecules are evaporated from the sample. Thus, we assign the third peak at 290°C observed in the pressure curve of Fig. 1a to the evaporation of the arsenic molecules product of Eq. (1).

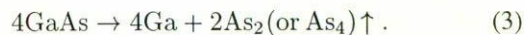
After the outgassing process we end with a thinner oxide layer principally composed of Ga_2O_3 . The changes in the chemical composition of the oxide at the end of this process are clearly observed in the AES results of Fig. 8. The increase in the O/As ratio after the outgassing is due to the loss of As according to Eq. (1). The loss of As is also observed by the increase of the Ga/As and the decrease of the As/(Ga+As) ratio. On the other hand, the apparent increase of the O/Ga ratio should be caused by the presence of the Ga_2O_3 layer near the GaAs surface, which can more efficiently contribute to the AES intensity after the thinning of the oxide layer at the end of the outgassing. Moreover, the bare GaAs surface could even be exposed in the regions rich on volatile As-oxides. This is supported by the appearance of GaAs diffraction spots at the end of this process (Fig. 6b). At higher temperatures this exposition will allow As to evaporate from the GaAs substrate, initiating the erosion on the sample surface. Contrary to this, on GaAs regions covered by the more stable Ga-oxides (like Ga_2O_3) the outgassing temperatures are not high enough to remove these oxides off the substrate. The proposed pit formation mechanism is consistent with the pressure behavior in Fig. 1a, where as explained before, the pressure variations are related to the desorbing species from the substrate. This is the first time, to our knowledge, that results demonstrate that the surface pits observed after the oxide removal have their origin at temperatures as low as 350°C , and second, that they are related to the desorption of highly volatile As-oxides.

During the second thermal process we expect the removal of the Ga-oxides. Yamada *et al.* [12], have reported the detection of the volatile Ga-oxide Ga_2O at the temperature of $\sim 400^\circ\text{C}$. Therefore, we assign the first peak centered at 410°C in the pressure curve of Fig. 2a to the evaporation of Ga_2O . On the other hand, when the substrate reaches temperatures up to $\sim 500^\circ\text{C}$ another chemical reaction occurs [12–14]:



From this equation it is important to point out that Ga from the substrate is required in order to reduce the most stable Ga-oxide Ga_2O_3 to Ga_2O . This is an unstable compound that at these temperatures is lost by sublimation, resulting in the second peak of the pressure curve of Fig. 2a.

Also, at these temperatures the GaAs molecule may break into its components Ga and As. Since As has a higher vapor pressure than Ga, is easily evaporated according to Eq. (3):



The great loss of As during the second thermal process is clearly observed by the increase of the Ga/As and the decrease of the As/(Ga+As) ratio shown in Fig. 8b.

From Eqs. (2) and (3) we propose that the As evaporation and the generation of free Ga are responsible for the elliptical shape of the surface pits shown in the Fig. 5, as follows.

In the early stages of the pits formation the loss of As leads to the generation of free Ga [Eq. (3)], which diffuses and contributes to the chemical reaction of Eq. (2), making possible the removal of the Ga_2O_3 oxide. Thus, this oxide removal process occurs with a preferential oxide etching rate depending on the diffusing behavior of Ga.

According to the AFM image of the Fig. 5 it results evident, from the elliptical shape of the voids, that the etching rate is predominant along the $[0\bar{1}1]$ direction over the $[011]$ direction. This fact is explained taken into consideration the diffusion length anisotropy of the free Ga. Many published papers have reported a longer Ga diffusion length on the $[0\bar{1}1]$ direction than on the $[011]$ for the GaAs(100) surface [15–17]. Thus, we are proposing that the final pits elliptical shape is influenced by this larger diffusion length of the free-Ga, which during the migration contributes in the preferential etching of the oxide layers along the $[0\bar{1}1]$ direction producing volatile species according to Eq. (2).

The pits have a density of $10^9/\text{cm}^2$ and it has been proved that they are not intrinsic defects of the GaAs surface revealed by the oxide desorption process because these voids are deeper than the oxide thickness formed on the surface of the samples by oxidation [14, 18]. The surface pits are a consequence of the high temperature oxide removal, this fact is corroborated by the AFM images shown in the Figs. 3a to 3c.

The presence of surface pits represents a serious problem to obtain high quality GaAs surfaces for epitaxy, since they may act as nucleation sites for crystal defects such as dislocations and stacking faults. Therefore, methods to obtain a smooth starting GaAs surface should be investigated.

Figure 9 is an AFM image of a GaAs substrate desorbed at $\sim 530^\circ\text{C}$ in a hydrogen radical flux. A significant difference can be observed comparing this image with that of the Fig. 3c. The rms roughness in Fig. 9 is 4.8 \AA . This value is about one order of magnitude smaller than the rms value of the sample shown in the Fig. 3c. The most important result is that voids are not observed on the GaAs surface of Fig. 9. This notorious difference in the surface morphology is due to the fact that H radicals induce distinct chemical reactions on the GaAs surface compared to samples desorbed in standard conditions. Under the influence of H radicals, Ga-oxides as long as As-oxides can be desorbed according with the follow-

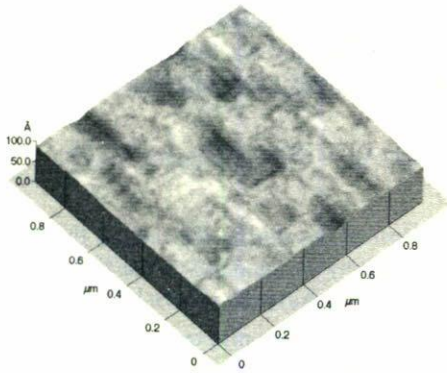


FIGURE 9. AFM image of the surface of a GaAs (100) substrate after the oxide desorption process assisted by a flux of hydrogen radicals.

ing chemical reactions [19, 20]:



where $x = 1, 3$ or 5 depending on the arsenic oxide, and



We think that the chemical reactions above indicated are responsible for the improvement in the GaAs surface morphology of the Fig. 9 (as compared to Fig. 3c). A very important point in the previous discussion is that Eqs. (4) and (5) clearly indicate that the removal of GaAs oxides does not

involve chemical reactions with the underlying Ga and As atoms. This fact could explain the improvement in the H-treated GaAs substrates, surface erosion is avoided. Further experiments to improve and optimize our results are underway.

5. Conclusions

The typical oxide desorption process used in MBE to clean GaAs substrates in UHV conditions promotes the generation of surface pits in a density of $10^9/\text{cm}^2$, increasing the roughening statistics observed on the GaAs surface by AFM. The pits can be as deep as 120 \AA according to the AFM images.

We present results demonstrating that surface pits have their origin at temperatures as low as 350°C , and it was found they are closely related to the evaporation of the most unstable As-oxides. On the other hand, when the temperature increases chemical reactions between the elements of the GaAs substrate and the oxides are favored. These chemical reactions lead to a stoichiometric degradation as well as surface erosion of the GaAs substrates. The use of a radical H flux during the oxides desorption process is a promising method to solve this problem.

Acknowledgments

The authors acknowledge the technical support of Rogelio Fragoso, Hector Silva, and Sonia Quintana. This work was partially supported by CONACYT-México.

1. S. Taniguchi *et al.*, *Electron. Lett.* **32** (1996) 552.
2. M. López-López, A. Guillen-Cervantes, Z. Rivera-Alvarez, and I. Hernández-Calderón, *J. Cryst. Growth* **193** (1998) 528.
3. S. Itoh, S. Tomiya, R. Imoto, and A. Ishibashi, *Appl. Surf. Sci.* **117/118** (1997) 719.
4. C.E.C. Wood *et al.*, *J. Appl. Phys.* **54** (1983) 2732.
5. J.H. Neave and B.A. Joyce, *J. Cryst. Growth* **44** (1978) 387.
6. C.W. Wilmsen, *Thin Solid Films* **39** (1976) 105.
7. C.W. Wilmsen, R.W. Kee, and K.M. Geib, *J. Vac. Sci. Technol.* **16** (1979) 1434.
8. J.P. Contour, J. Massies, H. Fronius, and K. Ploog, *Jpn. J. Appl. Phys.* **27** (1988) L167.
9. K. Bock, H.L. Hartnagel, and J. Dumas, *Reliability of Gallium Arsenide MMICS*, edited by A. Christou, (John Wiley and Sons Ltd, New York, 1992) Chapter 6.
10. C.D. Thurmond, G.P. Schwartz, G.W. Kammlott, and B. Schwartz, *J. Electrochem. Soc.* **127** (1980) 1366.
11. G.P. Schwartz, *Thin Solid Films* **103** (1983) 3.
12. M. Yamada and Y. Ide, *Surf. Sci.* **339** (1995) L914.
13. K. Tone, M. Yamada, Y. Ide, and Y. Katayama, *Jpn. J. Appl. Phys.* **31** (1992) L721.
14. G.W. Smith *et al.*, *J. Cryst. Growth* **127** (1993) 966.
15. M. López and Y. Nomura, *J. Cryst. Growth* **150** (1995) 68.
16. M. Hata, T. Isu, A. Watanabe, and Y. Katayama, *J. Vac. Sci. Technol. B* **8** (1990) 692.
17. X.Q. Shen and T. Nishinaga, *Jpn. J. Appl. Phys.* **32** (1993) L1117.
18. G.W. Smith *et al.*, *Appl. Phys. Lett.* **59** (1991) 3282.
19. Y. Ide and M. Yamada, *J. Vac. Sci. Technol. A* **12** (1994) 1858.
20. Y. Morishita *et al.*, *J. Cryst. Growth* **150** (1995) 110.